Iterative Change Detection Algorithm for Low-Frequency UWB SAR

Ricardo D. Molin Jr, Ana C. F. Fabrin, Pedro Sperotto, Dimas I. Alves, Fábio M. Bayer, Renato Machado, Mats I. Pettersson, Hans Hellsten, Patrik Dammert, Lars Ulander

***Abstract*— This paper presents an iterative change detection algorithm for low frequency UWB synthetic aperture radar (SAR) images. The proposed algorithm was compared in terms of false alarm rate (FAR) and probability of detection (P_D) to the method presented by the Swedish Defense Research Agency (FOI) [1]. The experimental analysis considered a set of 24 SAR images acquired in a military area of 6 km^2 in northern Sweden. The numerical results have shown that the proposed algorithm has a superior performance when compared to the algorithm proposed in [1].**

***Keywords*— SAR, CDA, CFAR, CARABAS**

I. INTRODUCTION

In the last two decades, the research on change detection methods on the Earth surface have been gaining prominence in remote sensing with current applications in deforestation surveillance [2], urban surveillance [3] and for military applications [1], [4]. Synthetic aperture radar (SAR) provides high-resolution imagery, even at night or with bad weather conditions due to a synthetic aperture formed by a moving satellite or aircraft, which simulates a physical antenna of several times its real size.

SAR systems are widely used to generate high-resolution maps based on the relative motion between the antenna and the imaged scene [5]. There is a series of challenges related to the SAR imagery system, including aircraft integration of the antenna system, frequency allocation and sharing of common bands. Most of these problems have already been explored, but a breakthrough of the technology still awaits a robust detection mechanism [6].

The main challenge in the design of a change detection method consists of sufficiently suppress the clutter to give a false alarm rate (FAR) low enough to be useful to the operator [1]. Such suppression is obtained by forming a single image from the differences between two or more images from the same area, acquired at different times.

In [1] the Swedish Defence Research Agency (FOI) has made public a set of data regarding the acquisition of SAR images from a military zone in northern Sweden, as well as the results from a baseline change detection algorithm, in order to encourage the development of new models. The data consists of a set of 24 SAR images acquired by CARABAS-II system and can be found in [1]. The images contain only amplitude information and illustrate a densely forested area of 3×2 km^2 where 25 military vehicles were concealed under foliage. The radar system operates at the VHF-band, 20-90 MHz, which means that the emitted wavelength are sufficiently high to penetrate the foliage [6].

In this context, the focus of this paper resides in the detection of military vehicles concealed by dense vegetation. The detection is based on the change detection concept by using two SAR images in an offline post-processing analysis. The proposed change detection algorithm is able to detect targets with different amplitude levels. The algorithm is based on an iterative method inspired by the control chart application, which is a tool of the statistical process control [7], [8]. The proposed method is able to discriminate pixels that represent targets from the ones that represent only forest. Numerical results show that the proposed iterative algorithm has a better performance when compared to the one presented in [1].

The remainder of this paper is organized as follows. In Section II, the database used in this work is presented. Section III describes the proposed algorithm. In Section IV, the numerical results are presented. Finally, Section V gives some final remarks.

II. DATA DESCRIPTION

The detection problem of military vehicles in dense vegetation discussed in this paper exploits SAR images obtained in 2002 in a forest area with predominance of pine trees located in northern Sweden [1]. The imaged area of 6 km^2 includes rivers, fences, roads and trees with large trunks, a fact that hinders the detection of targets through a single image. The vehicles are arranged in this region, and are distributed in a manner approximately uniform in order to facilitate their identification in tests.

The data acquisition was performed by the CARABAS-II SAR system [1], which was coupled to a Sabreliner aircraft in a nominal altitude of 3000 m, operating in the low-VHF

R. D. Molin Jr, A. C. F. Fabrin, P. Sperotto, Communications and Signal Processing Research Group, Department of Electronics and Computing, Federal University of Santa Maria, 97105-900, Santa Maria-RS, Brazil. E-mails: {ricardosddj, fabrin.anacarolina, ph.sperotto}@gmail.com. D. I. Alves, Communications and Signal Processing Research Group, Federal University of PAMPA, 97546-550, Alegrete-RS, Brazil. F. M. Bayer, Departament of Statistics and Space Science Laboratory of Santa Maria, CRS-INPE, Federal University of Santa Maria, 97105-900, Santa Maria-RS, Brazil. E-mail: fabiobayer@gmail.com. R. Machado, Communications and Signal Processing Research Group, and Space Science Laboratory of Santa Maria, CRS-INPE, Department of Electronics and Computing, Federal University of Santa Maria, 97105-900, Santa Maria-RS, Brazil. E-mail: renatomachado@ufsm.br. M. I. Pettersson, Blekinge Institute of Technology, Karlskrona, SE-371 79, Sweden. E-mail: mats.pettersson@bth.se. H. Hellsten and P. Dammert, Systems Design - Saab Electronic Defence Systems, SE-412 89 Gothenburg, Sweden. E-mail: {patrik.dammert, hans.hellsten}@saabgroup.com. L. Ulander, Swedish Defence Research Agency - FOI, Linköping, SE-581 11, Sweden. E-mail: lars.ulander@foi.se.

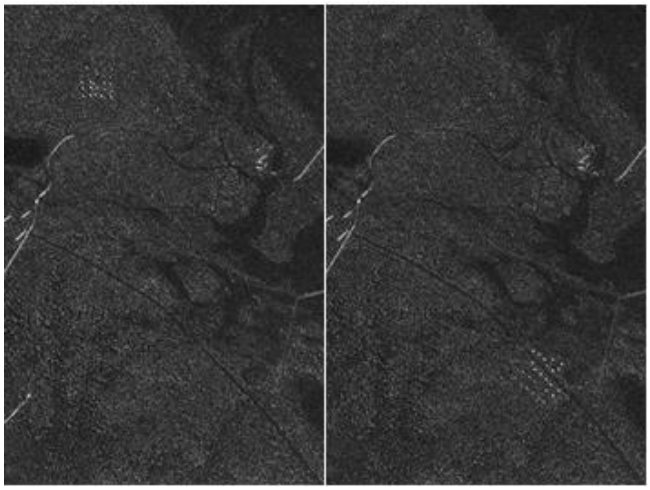

Fig. 1. Example of a pair of images used in this study. Each image can be represented as a matrix of 3000 × 2000 pixels, which corresponds to an area of 6 km^2.

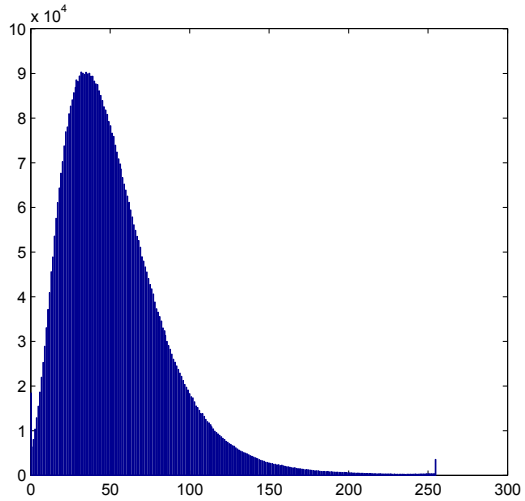

Fig. 2. Histogram of one of the considered images.

frequency range 20-90 MHz. The choice of the operating frequency is such that both extinction and backscatter from the foliage are favourably small whereas the radar-cross section (RCS) of the targets is favourably high [6]. This frequency band assures that only objects of 1 m or larger are visible in the images, in a way that the majority of the changes that occur in nature, such as falling leaves or twigs and animal movements, are not registered in the imagery. The terrestrial targets, on the other side, consisted of 25 medium- and large-sized military vehicles, being ten TGB11, eight TGB30 and seven TGB40, with dimensions (length × width × height) $4.4 \times 1.9 \times 2.2$ m, $6.8 \times 2.5 \times 3$ m, and $7.8 \times 2.5 \times 3$ m, respectively [1].

The SAR images that were the object of study in this paper were formed through a process of fast factorized back-projection [5]. The raw radar data have already been calibrated [9], filtered and equalized [6] and georegistered [10]. In order to illustrate the images we are using in this work, one of the base pairs employed in this study is shown in Fig. 1. In the left image, the targets can be seen in the upper-left corner; and in the image on the right, the targets are grouped in the lower-right corner. Although the targets appear as highlighted points in Fig. 1, other structures, such as fences, roads and power lines are also prominent, making it difficult to correctly detect the targets.

In terms of change detection there is a series of techniques employed in the change image formation, which can be based on pixel, object or spatial data mining [11]. The pixel-based techniques are widely used in change detection and are attractive by their simplicity and the possibility of direct comparison between images. Among these, there is the image differencing method, which offers easy interpretation of results and has been used successfully in change detection in forest areas [12]. This approach, however, has the disadvantage of detecting isolated pixels [13] and difficulty in choosing an optimal threshold [14]. Such problems are circumvented in [1] with the use of morphological operations at the end of the detection and for the generation of a receiver operating characteristics (ROC) curve [15]. This methodology is also adopted in this paper. The employment of the differencing technique is yet supported by the fact that we are using real images, i.e., the images contain only amplitude information, since the phase has been removed [1].

Each pixel represents an area of 1 m × 1 m, in such a way that the SAR images are arrays of 3000 rows by 2000 columns. Besides, we exploit JPEG imagery with 8 bits of information, which means that each element assumes values from 0 to 255, with the targets found at the highest amplitudes. The histograms of the images show distributions close to Rayleigh [16], as illustrated in Fig. 2.

From the data collected by the CARABAS-II system [1], a subset of 24 images from four different missions, each associated with a different target deployment, was released by the FOI to encourage the development of new change detection algorithms in VHF SAR imagery. For each mission, six images were registered, from three flight directions. We adopt the notation M_D, to represent the mission M and its image D.

In this paper, we propose an iterative change detection method with a pixel-based approach, which can be considered efficient in processing, since pre-filtering is not employed, the change image is calculated simply by differencing and the image data is entirely normalized, resulting in an algorithm with simple and few calculations and with great potential in monitoring areas covered by vegetation.

III. Iterative Change Detection Algorithm

In this section we describe the proposed iterative change detection algorithm. First, we combine two SAR images, then a differencing technique is applied, which is given by

$$\mathbf{I_d}[\mathbf{i},\mathbf{j}] = \mathbf{I_1}[\mathbf{i},\mathbf{j}] - \mathbf{I_2}[\mathbf{i},\mathbf{j}],$$

where $\mathbf{I_1}$ and $\mathbf{I_2}$ are two images from the same area, but different missions, i.e. acquired at different times, and $[i,j]$ are the coordinates expressed in line ($i = 1, 2, \ldots, 3000$) and column ($j = 1, 2, \ldots, 2000$). Therefore, the change image $\mathbf{I_d}$ contains pixels that are distributed around zero, where

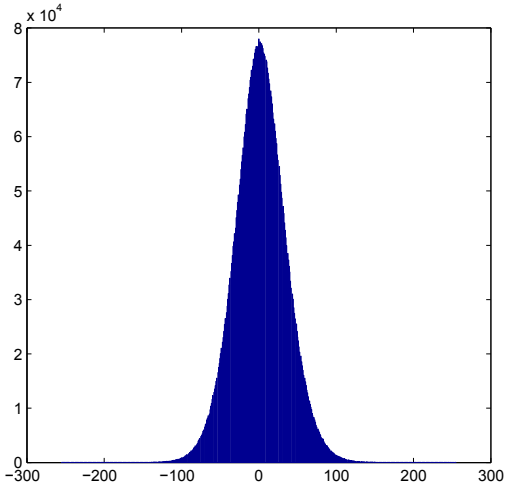

Fig. 3. Histogram of the change image for a considered pair.

no change occurs, and pixels located in the tails of the distribution, where the change is present [17]. Besides, the change image has i) positive values, when an object becomes present in a certain area, and ii) negative values, when an object is removed from this place. Additionally, values from the entire amplitude range (-255 to 255 in the change image) are affected by noise, clutter and other conditions during the imagery acquisition of the images. Even though the images were equalized and georeferenced with a GPS, the images present significant information differences, in such a way that the output image from the differencing process has an approximately normal distribution, as shows the histogram in Fig. 3. This difference image is the input of the proposed algorithm.

The motivation for the proposed method comes from [7], [18]. The control charts are the main tools from the statistical process control [7], [8] whose goal is to distinguish common (random) causes from special causes in an observed stochastic process. Likewise, in target detection the goal is to separate random variabilities (no change) from nonrandom variabilities (change). Like in the applications of control charts [18], we introduce an iterative series of steps until appropriate thresholds are defined, in which every pixel within these thresholds, i.e. smaller than absolute 6, are considered random. Pixels with greater magnitudes than these thresholds are considered targets.

Given a change image $\mathbf{I_d}$, the proposed algorithm is described as follows:

1) Calculate the mean and standard deviation of the change image, given, respectively, by

$$\hat{\mu} = \frac{1}{N+M}\sum_{i=1}^{N}\sum_{j=1}^{M}\mathbf{I_d}[\mathbf{i},\mathbf{j}],$$

$$s = \frac{1}{N+M-1}\sum_{i=1}^{N}\sum_{j=1}^{M}\left(\mathbf{I_d}[\mathbf{i},\mathbf{j}]-\hat{\mu}\right)^2,$$

where $N = 3000$ and $M = 2000$ are the total number of lines and columns, respectively.

2) Determine the lower and upper thresholds

$$\mathrm{LI} = \hat{\mu} - k\cdot s,$$
$$\mathrm{LS} = \hat{\mu} + k\cdot s,$$

where k is a constant expressed in units of standard deviation. In this paper, we adopt $k = 6$, due to the data characteristics.

3) For each pixel $[i,j]$ it is verified if $\mathrm{LI} \le \mathbf{I_d}[\mathbf{i},\mathbf{j}] \le \mathrm{LS}$. If $\mathbf{I_d}[\mathbf{i},\mathbf{j}]$ is out of the interval $[\mathrm{LI},\mathrm{LS}]$, then this pixel is removed and the program returns to step 1).
4) Steps 1), 2) e 3) are repeated until every scanned pixel is inside the interval $[\mathrm{LI},\mathrm{LS}]$.

By the end of the iterative process, a binary image is created with value 1 assigned to the pixels outside the interval $[\mathrm{LI},\mathrm{LS}]$ (change) and 0 to the remainder (no change) [17].

In the same way as in [1], after the pixel detection algorithm, some morphological operations are carried out in order to remove detections considered too small, based on the system resolution (approximately 3 m for our database), and to merge the ones that are part of a single target. Isolated pixels are immediately discarded, and the remainder dilated. The ones that do not merge with any group of pixels and still do not comply with the system resolution are removed as well. The final detection is then performed by object and the targets coordinates are given by their central point.

We call attention to the fact that the threshold $k = 6$ applied in the proposed algorithm is the same as in [1], preliminary defined for comparison purposes. Post-detection tests through a ROC curve show that this threshold is close to an optimum value.

IV. Numerical results

The proposed algorithm was tested in the same set of images used in [1] and already discussed in Section II. The performance of the presented algorithm was evaluated th-rough comparisons with the results of the detection algorithm published in [1]. The method proposed in [1] considers a likelihood ratio test assuming normal distribution to the change image formation, followed by a FAR normalization filter [1], which provides an appropriate threshold.

The primary performance measurements in the analysis of target detection are the probability of detection (P_D) and FAR. These measurements can be defined, respectively, by:

$$\mathrm{P}_D = \frac{\text{Number of detected targets}}{\text{Total number of targets}},$$

$$\mathrm{FAR} = \frac{\text{Number of false alarms}}{\text{km}^2}.$$

A target is considered correctly detected when is found within a radius of 10 meters from the ground truth position, or in terms of processing analysis, within a radius of 10 pixels, as defined in [1]. Detections beyond this radius are counted as false alarms.

Results show that in 15 of the pairs the proposed change detection algorithm exhibited superior performance, in 2 of them inferior and in 7 the P_D was greater with a less

TABLE I

PERFORMANCE COMPARISON BETWEEN THE PROPOSED METHOD AND THE ONE PRESENTED IN [1]

Measurements	FOI [1]	Proposed
P_D	97%	95.5%
FAR	67%	20.83%

TABLE II

RESULTS IN TERMS OF DETECTION AND FALSE ALARM FOR SIX SELECTED PAIRS OF IMAGES.

Surveillance image	Reference image	Detected targets		False alarms	
		FOI [1]	Proposed	FOI [1]	Proposed
2_1	3_1	25	25	2	0
3_1	4_1	22	23	1	7
3_3	2_3	23	24	4	0
4_4	5_4	25	25	4	2
5_1	2_1	23	24	4	4
5_6	4_6	23	24	3	0

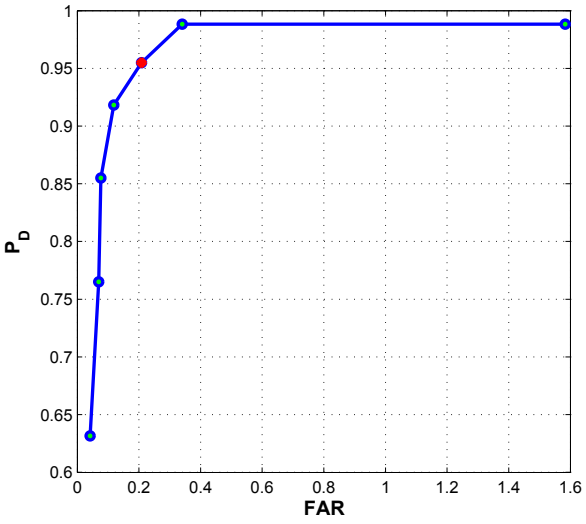

Fig. 4. ROC curve of the proposed iterative algorithm for different values of k. The highlighted point in red corresponds to k = 6.

favourable FAR or vice versa. In general terms of performance, the proposed algorithm reduced the FAR in more than three times, with almost the same P_D, as shown in Table I. Table II presents part of the obtained results for six selected pairs of images.

The proposed detection algorithm has shown, overall, better results. However, for some pairs of images a higher FAR is noticed, which is the case of the second pair (3_1 in relation to 4_1, for missions 3 and 4) shown in Table II. This pair, which can be seen in Fig. 1, presents in the monitored image much more significant pixels in terms of amplitude than the reference image of the same region. These pixel groups, when dilated, do not merge to form a single detection. The algorithm proposed here focuses on the detection of atypical points in the distributions, and does not take into account in this preliminary version the shape or maximum dimension of a set of pixels in a neighbourhood.

The main contribution of the change detection method proposed here is the possibility of detecting groups of targets situated in lower levels of amplitude than the ones that were previously detected. Such process mitigates the limitations of defining an optimum threshold and allows the detection of targets found, for example, in an area with denser vegetation where no targets were found in a first moment. This characterizes the method as adaptive, being flexible for applications in different scenarios.

The evaluation of the conformity of the threshold in detection problems can be formulated through the analysis of an ROC curve, which shows the probability of detection as function of the false alarm rate for different thresholds. The P_D and FAR parameters can be inferred from the tests on account of the previous knowledge of the targets coordinates. Hence, we investigated the impact of different values for the constant k in the performance of this method. For this paper, we considered values of k belonging to the following set of values: $\{5, 5.5, 6, 6.25, 6.5, 6.75, 7\}$. The results from this evaluation can be seen in Fig. 4. The point highlighted in red corresponds to k = 6. As we look for a high P_D and low FAR, an optimum threshold is found on the upper-left region of the ROC curve [15].

In this context, the employment of a threshold k = 6 is supported by the ROC curved based on the iterative algorithm presented here. The analysis of Fig. 4 shows that the applied threshold in the algorithm presents a decent performance in terms of its parameters P_D and FAR.

V. CONCLUSIONS

In this paper, an iterative change detection algorithm for low-VHF SAR system has been proposed. The proposed method was evaluated through computer simulations using a set of 24 images [1]. In comparison to the performance of the proposed method was considered the method presented in [1]. Results have shown that the FAR has been reduced from 67%, exhibited by the baseline algorithm, to 20,83% for the proposed one. In terms of P_D the proposed algorithm presented comparable results (97% × 95,5%). In this way, the proposed algorithm presented an overall better performance in the final solution for most of the images pairs. In addition, the proposed method is very simple and computationally efficient. The repeatability of the method offers great potential for the detection of groups of targets with different levels of amplitude, either by the characteristics of their own or the vegetation where they are found. Therefore, the preliminary results show that the proposed algorithm has good performance, but more efforts must be made in order to improve the algorithm performance.

ACKNOWLEDGEMENTS

The authors would like to thank the Swedish Defence Research Agency (FOI) for providing the CARABAS-II SAR data, the Brazilian National Council for Scientific and Technological Development (CNPq), the Swedish-Brazilian Research and Innovation Centre (CISB), the Brazilian Army and SAAB AB for the financial support.

REFERENCES

[1] M. Lundberg, L. M. H. Ulander, W. E. Pierson, and A. Gustavsson, "A challenge problem for detection of targets in foliage," *Proceedings of SPIE*, 2006.

[2] R. A. Filho, A. Rosenqvist, S. Y. E., and R. S. Gomez, "Detecting deforestation with multitemporal l-band SAR imagery: a case study in western brazilian amazônia," *International Journal of Remote Sensing*, vol. 28, no. 6, pp. 383–390, 2007.

[3] F. M. Henderson and Z. G. Xia, "SAR applications in human settlement detection, population estimation and urban land use pattern analysis: a status report," *IEEE Transactions on Geoscience and Remote Sensing*, vol. 35, no. 1, pp. 78–85, 1997.

[4] T. S. Levitt, C. L. Winter, C. J. Turner, R. A. Chestek, G. J. Ettinger, and S. M. Sayre, "Bayesian inference-based fusion of radar imagery, military forces and tactical terrain models in the image exploitation system/balanced technology initiative," *International Journal of Human-computer Studies*, vol. 42, no. 6, pp. 667–686, 1995.

[5] L. M. H. Ulander, H. Hellsten, and G. Stenström, "Synthetic-aperture radar processing usin fast factorized back-projection," *IEEE Transactions on Aerospace and Electronic Systems*, vol. 39, no. 3, pp. 760–776, 2003.

[6] L. M. H. Ulander, P. O. Frölind, A. Gustavsson, H. Hellsten, and B. Larsson, "Detection of concealed ground targets in CARABAS SAR imagens using change detection," *Proceedings of SPIE*, pp. 243–252, 1999.

[7] D. C. Montgomery, *Introduction to Statistical Quality Control*, 6th ed. John Wiley & Sons, Inc., 2009, no. 4.

[8] J. S. Oakland, *Statistical Process Control*, 6th ed. Routledge, 2007.

[9] L. M. H. Ulander, P. O. Frölind, and T. Martin, "Processing and calibration of ultra-wideband SAR data from CARABAS-II," *SAR workshop: CEOS Committee on Earth Observation Satellites*, vol. 450, p. 273, 1999.

[10] F. Walter, J. E. Fransson, and P. O. Frölind, "Fully automatic geo-coding of CARABAS-II VHF SAR images," *Proceedings IGARSS*, vol. 1, pp. 569–573, 1999.

[11] M. Hussain, D. Chen, A. Cheng, H. Wei, and D. Stanley, "Change detection from remotely sensed images: From pixel-based to object-based approaches," *ISPRS Journal of Photogrammetry and Remote Sensing*, vol. 80, pp. 91–106, 2013.

[12] P. R. Coppin and M. E. Bauer, "Digital change detection in forest ecosystems with remote sensing imagery," *Remote Sensing Reviews*, vol. 13, no. 3-4, pp. 207–234, 1996.

[13] S. Bontemps, P. Bogaert, N. Titeux, and P. Defourny, "An object-based change detection method accounting for temporal dependences in time series with medium to coarse spatial resolution," *Remote Sensing of Environment*, vol. 112, no. 6, pp. 3181–3191, 2008.

[14] J. Jensen, *Introductory Digital Image Processing: A Remote Sensing Perspective*, U. S. River, Ed. Prentice Hall, 2005.

[15] C. E. Metz, "Basic principles of ROC analysis," *Seminars in Nuclear Medicine*, vol. 8, no. 4, pp. 283–298, 1978.

[16] E. E. Kuruoglu and J. Zerubia, "Modeling SAR images with a generalization of the Rayleigh distribution," *IEEE Transactions on Image Processing*, vol. 13, no. 4, pp. 527–533, 2004.

[17] A. Singh, "Review article digital change detection techniques using remotely-sensed data," *International Journal of Remote Sensing*, vol. 10, no. 6, pp. 989–1003, 1989.

[18] L. A. Jones and C. W. Champ, "Phase I control charts for times between events," *Quality and Reliability Engineering International*, vol. 18, no. 6, pp. 479–488, 2002.